Contribution from the Research Laboratories,
Eastman Kodak Company, Rochester, New York 14650

Calculated Properties of CuCl and Na Clusters

R. C. BAETZOLD* and R. E. MACK

Received June 21, 1974 AIC404012

Semiempirical molecular orbital calculations for small $(CuCl)_n$ and Na_n clusters (n = 1, ..., 15) have been performed. The bond energy, ionization potential, geometry, and excitation energy are in good agreement with experimental values. These properties are quite different from bulk properties. Small clusters exhibit higher ionization potential and excitation energy but lower bond energy. The most stable geometries calculated do not have the largest average coordination number.

I. Introduction

Recently there has been increasing interest in the calculation of electronic properties of clusters containing transition elements. Semiempirical techniques, such as complete neglect of differential overlap[1] (CNDO) and extended Hückel[2] (EH) are generally available and have been employed for this purpose. The reasons for this interest are based upon the possibility of metallic bonding in small clusters, which is amenable to experimental study by a variety of physical–chemical techniques. Practical use of such information is important, for example, in the field of catalysis, where small clusters of supported transition metals show unusual catalytic properties.[3,4] In addition, the electronic properties[4] of clusters of atoms are important in nucleation where bonding energies determine stable configurations.[5]

The semiempirical molecular orbital procedure has been applied to the metal cluster problem. Other less approximate calculational procedures involve so many complex integrals that they are generally not feasible on present computers. Recent calculations have treated Li and Be clusters,[5] C particles,[6] Fe chains,[7] and Ni clusters.[8] In all cases the electronic properties of the small cluster are somewhat different from bulk properties. We found in the case of Ag[9,10] a significant gap between highest occupied and lowest unoccupied energy levels unlike the spacing $\sim kT$ found in the bulk. The gap decreases with size, approaching 0.5 eV for linear 20-atom silver particles. In addition, the geometry of small particles may be quite unexpected. Calculations have shown the low-energy form of small clusters of Ag, Li, and Cd to be linear chains. The ionization potential of Ag clusters decreases from its single-atom value toward the bulk work function as cluster size increases. Palladium clusters[9] were calculated to possess vacant d molecular orbitals increasing in number with cluster size. Clusters of other atoms, such as Cd and Ni,[10] have been investigated using these methods and possess electronic properties intermediate between single-atom and bulk-metal properties. In addition to these calculations, the methods have been applied to treat adsorption of species on metal substrates such as Ni[11,12] and Pb.[13]

The question arises as to the reliability of the foregoing MO techniques for predicting properties of clusters containing metal atoms. The general paucity of experimental data for such small clusters makes comparisons of experiment and calculation difficult. Calculations of transition energies in heavy metal complexes,[14] such as VO^{2+}, have indicated that the MO methods are generally useful. Recently, experimental information on geometry, bond energy, ionization potential, and bond length for $(CuCl)_n$ for the series n = 1, ..., 5 has become available.[15,16] In addition, ionization potentials for Na_n, n = 1, ..., 8, have been measured.[17] The newer data in both of these systems are measured by a mass spectrometric technique for the vapor-phase species. The availability of these data offers the possibility of testing the MO techniques on metal atom systems for several electronic parameters. We believe this type of test is important in gauging the reliability of the MO techniques for such systems.

Table I. CNDO Input Parameters

Atom	Orbital	½(IP + EA), eV	β°	Slater exponent
Cu	4s	−4.445	−2	0.84
	4p	−2.555	−2	1.46
	3d	−5.955	−2	2.35
Cl	4s	−2.530	−5	1.36
	3p	−8.320	−5	1.36
Na	3s	−2.610	−1	0.84
	3p	−1.560	−1	0.84

II. Calculational Procedure

A. CNDO. The CNDO procedure developed by Pople, *et al.*,[1] and applied to transition metal atoms by us[18] has been employed in these calculations. Since the standard procedure is well known, it will not be repeated except for the expression used for diagonal F matrix elements given in eq 1.

For s orbitals we employ

$$F_{\mu\mu} = -{}^1/_2(IP_s + EA_s) + \gamma_{ss}^{AA}(-N_A + 0.5 + P_{ss}^{AA} - 0.5P_{\mu\mu}) + (P_{dd}^{AA} - M_A)\gamma_{sd}^{AA} + \sum_{B \neq A} [(P_{ss}^{BB} - N_B)\gamma_{ss}^{AB} + (P_{dd}^{BB} - M_B)\gamma_{sd}^{A,B}] \quad (1)$$

where IP_s = ionization potential for s orbital, EA_s = electron affinity for s orbital, N_A = number of s and p electrons on atom A, M_A = number of d electrons on atom A, $P_{\mu\nu}$ = bond density element, P_{ss}^{BB} = sum of $P_{\mu\mu}$'s for s orbitals on atom B, $S_{\mu\nu}$ = overlap matrix element, and $\gamma_{\mu\nu}^{A,B}$ = repulsion integral between orbital μ on atom A and orbital ν on atom B. An analogous expression for d orbitals can be obtained by interchanging s with d, N_A with M_A, and N_B with M_B in eq 1. Values of the repulsion integrals were calculated for s and p orbitals using s-orbital exponents so that $\gamma_{ss} = \gamma_{sp} = \gamma_{pp}$ was preserved. As in all approximate calculations of this type, Slater s orbitals with proper exponents are used to calculate the repulsion integrals whether they involve s, p, or d orbitals. Experimental values for EA and IP were employed when available from atomic tables.[19] Values of EA were estimated based upon IP differences for orbitals where no experimental data exist. The iterative procedure was carried out such that input and output charge for each atom differ by less than 0.01 as a criterion for convergence.

The atomic parameters used in these calculations are listed in Table I. Experimental ionization potentials and electron affinities were used, as well as Slater orbitals employing Clementi exponents[20] or matching overlap exponents.[21] The resonance parameter β° used for each element in CNDO was determined by fit of calculated to experimental data for the homonuclear diatomic molecules. Table II shows the degree of fit obtained for Cl_2 and Cu_2 using the best choice of β° and gives an indication of the qualitative nature of these calculations. Calculated bond lengths are too large, but since all

Table II. Calculations *vs.* Experimental Data

Quantity	Cu_2		Cl_2	
	Calcd	Exptl	Calcd	Exptl
R_{eq}, Å	3.0	2.22[a]	2.9	2.00[d]
BE, eV	2.2	1.98[a]	3.1	2.48[d]
IP, eV	8.4	<6.7[b]	16.2	13.2[e]
ΔE, eV	2.8	2.70[c]	4.7	2.24[d]

[a] G. Verhaegen, F. E. Stafford, P. Goldfinger, and M. Ackerman, *Trans. Faraday Soc.*, 58, 1926 (1962). [b] P. Schissel, *J. Chem. Phys.*, 26, 1276 (1957). [c] B. Cleman and S. Lindkvist, *Ark. Fys.*, 8, 333 (1954). [d] G. Herzberg, "Molecular Spectra and Molecular Structure," Vol. I, 2nd ed, Van Nostrand, New York, N. Y., 1950, p 519. [e] "Handbook of Chemistry and Physics," 41st ed, Chemical Rubber Publishing Co., Cleveland, Ohio, 1959, p 2551.

Table III. Calculated Electronic Properties of $(CuCl)_n$ Clusters

Size	Geometry	Equilibrium bond length, Å	Av coord no.	BE/*n*, eV
2	Square, alternate	3.25	2	4.67
	Square, adjacent	3.30	2	3.55
	Straight chain	3.20	1.5	4.30
	Pyramid	3.30	4	3.85
	105° rhombus[a]	3.25	2	4.60
3	120° ring (symmetric)	3.25	2	4.81
	150° ring[a]	3.20	2	4.63
	Straight chain	3.20	1.67	4.40
	Octahedron	3.30	4	4.01
	Double chain	3.25	2.3	4.80
4	Cube	3.35	3	5.03
	Straight chain	3.10	1.75	4.50
	Symmetric ring	3.20	2	4.85
	Distorted cube[a]	3.35	3	4.83
5	Straight chain	3.30	1.8	4.63
	Symmetric ring	3.20	2	4.62
	Double chain	3.30	2.6	4.95
	Planar naphthalene structure	3.20	2.2	4.84
	90° distorted naphthalene	3.20	2.2	4.70
	Bicapped cube	3.30	4	4.36
6	Straight chain	3.30	1.83	4.68
	Bicubic	3.30	3.33	5.12
	Double chain (6 × 2)	3.30	2.67	4.99
	Flat surface (4 × 3)	3.30	2.83	4.98
	Hexagonal prism	3.30	3.0	5.11
7	Straight chain	3.20	1.86	4.71
	Double chain (7 × 2)	3.30	2.71	5.01
	Anthracene structure	3.30	2.30	4.75
8	Tricubic	3.30	3.5	5.17
	Zinc blende	3.56	2.3	4.51
	Double chain (2 × 8)	3.00	2.75	4.26
	Planar bioctagon	3.30	2.13	5.13
12	Multiple cubic	3.30	3.83	5.22
15	Multiple cubic	3.30	3.93	5.25

[a] Experimental cluster.

of these data are evaluated at the minima of potential energy curves, we chose not to attempt to improve this fit. Bond energies (BE), ionization potentials (IP), and energy of first excitation (ΔE) are calculated by energy difference of the appropriate initial and final systems for these CNDO calculations.

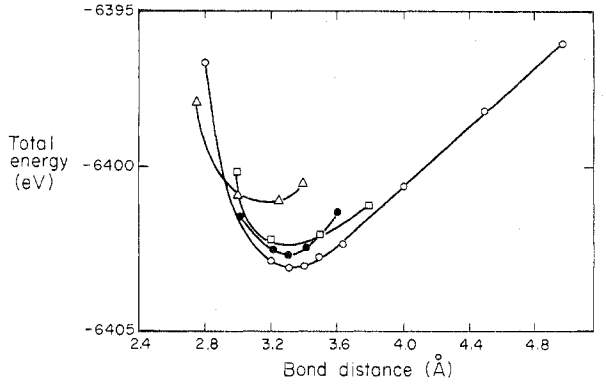

Figure 1. Potential energy *vs.* bond distance curve for various configurations of $(CuCl)_4$: △, straight chain; □, distorted cube; ○, regular cube; ●, ring. The energy of all the separated atoms in this system totals −6383.00 eV, making the bond energy of the regular cube 20 eV.

B. Extended Hückel. The extended Hückel procedure employed originally by Hoffmann[2] was used for Na cluster calculations. We employed a noniterative procedure in which either the Cusachs[22] formula or Wolfsberg–Helmholz[23] formula was used to calculate the off-diagonal Hamiltonian matrix elements.

III. Results

A. $(CuCl)_n$Clusters. 1. Bond Energy. Potential energy curves have been calculated for various $(CuCl)_n$ geometries, keeping all bond lengths constant in order to determine the equilibrium properties of these systems. Curves shown for $(CuCl)_4$ in Figure 1 are typical of the data that we obtained. The order of stability here is cube > symmetric ring > straight chain, but this order is not always found for other size clusters. Table III lists calculated bond energies per CuCl unit for various cluster sizes and geometries that we examined. The bond energy per CuCl unit is a gradually increasing function of size for the most stable clusters, indicating a trend to cohesion. For the clusters $n \leq 5$, all orbitals listed in Table I were included, but for larger clusters the Cu 4d orbitals were omitted. While symmetric rings are more stable for $n = 2$ or 3, the three-dimensional structures have increased stability at larger sizes. There does not seem to be a correlation between average coordination number and bond energy for the data in Table III, contradicting usual intuitive concepts, such as the pairwise additive principles embodied in classical bond potential descriptions of small clusters.[24] Structures with smaller than the maximum coordination number have the greatest stability for the small clusters, although we note that average coordination number of the most stable structure increases as cluster size increases.

2. Comparison with Experiment. The calculated data for the low-energy $(CuCl)_n$ cluster are compared to experimental data in Table IV. The CNDO procedure parameterized to fit Cu_2 and Cl_2 experimental data gives good agreement for CuCl data. Geometries are predicted with general accuracy, but the finer details, such as distortions from symmetric structures, are incorrect. Bond lengths are consistently 50% too large. Bond energies, ionization potentials, and energies

Table IV. Calculated *vs.* Experimental Quantities for $(CuCl)_n$

n	Equilibrium geometry		R_{eq}, Å		BE/*n*, eV		IP, eV		ΔE, eV	
	Calcd	Exptl	Calcd	Exptl	Calcd	Exptl	Calcd	Exptl	Calcd	Exptl
1	Linear	Linear	3.00	2.05	4.15	3.94	10.90	10.7	4.70	3.12
2	Square	75–105 rhombus	3.25	2.11	4.67	4.91	10.30	9.6	4.70	
3	120° ring	90–150° ring	3.25	2.16	4.81	5.62	10.30	9.9	5.31	5.54
4	Cube	Distorted cube	3.35	2.19	5.03	5.74	10.34	9.9	6.72	5.67
5	Double chain		3.30		4.95	5.75	9.74	9.7	5.31	
5	Planar bihexagon		3.20		4.85	5.75	11.97	9.7		

Table V. Calculated Electronic Properties of Na Clusters–CNDO

Size	Geometry	R_{eq}, Å	BE/n, eV	IP, eV
2	Linear	3.4	1.09	4.94
3	Linear		Unstable	
	Triangle	3.6	0.65	3.82
4	Square	3.8	0.76	
	Pyramid	4.2	0.79	
	Linear	3.8	0.97	5.35
5	Linear	4.0	0.76	3.54
6	Bipyramid	4.4	0.70	5.00
	Linear	4.0	0.93	5.03
7	Linear	4.0	0.79	3.39
8	Linear	4.0	0.91	4.84
	Cube	4.2	0.79	4.70

Table VI. Calculated Electronic Properties of Na Clusters–EH

Size	Geometry	R_{eq}, Å	BE/n, eV	IP(HOMO), eV
2	Linear	3.60	0.90	6.04
3	Linear	3.90	0.81	5.28
	Triangle	4.00	0.70	4.48
4	Linear	3.90	0.94	5.76
	Pyramid	4.25	0.63	4.72
5	Linear	4.00	0.91	5.28
	Bipyramid	4.50	0.70	4.85
6	Linear	3.75	0.96	5.62
	Bipyramid	4.50	0.76	5.32
7	Linear	3.75	0.95	5.29
8	Linear	3.80	0.98	5.56
	Cube	4.25	1.02	5.56

of excitation are predicted with good accuracy for the $(CuCl)_n$ clusters, falling within 10–20% of the experimental values. The general trends of these experimental properties *vs.* size are correctly followed by the calculated properties. Since we feel some reservation toward the double chain as the most stable structure for $(CuCl)_5$, data for a planar bihexagon are also included in Table IV.

3. Comparison with Bulk Properties. The calculated data for $(CuCl)_n$ clusters are considerably different from experimental data for bulk CuCl. The bulk structure is the zinc blende type having an average coordination number of 4, which is larger than the values of coordination number found for the most stable small clusters. The calculations for a $(CuCl)_7$ cluster in the zinc blende geometry determine an equilibrium distance 50% greater than bulk experimental, as found for the other clusters. The calculated BE/n is 4.65 eV compared with 9.63 eV for bulk experimental.[25] The band gap reported[26] for bulk CuCl is 3.3 eV, which is considerably less than the excitation energy 5.59 eV calculated for the zinc blende model. The trends in BE/n in Tables III and IV indicated an increase with increasing size, but apparently the small clusters are much less stable per CuCl unit than the bulk. The larger energy gap calculated for the small clusters may indicate a considerable difference in bonding between small CuCl clusters and bulk. Using the present approach for small clusters, we find that the Cu 4d orbitals are lower in energy than the 3p of Cl as opposed to recent ESCA experiments[27] on bulk CuCl showing the reverse.

Electrons are transferred from 4s orbitals of Cu to 3p orbitals of Cl. The average charge per ion calculated by a Mulliken-type analysis increases from 0.60 for $n = 1$ and 0.70 for $n = 2$ to 0.85 for $n = 3$. This indicates a considerably ionic bond for the small CuCl clusters much unlike the bulk CuCl, which is thought to be more covalent. Undoubtedly, the value of the charge is strongly related to the parameters chosen as input. These findings may be compared with those of Ros and Schuit,[28] who performed iterative Wolfsberg–Helmholz calculations for various geometries of $CuCl_4^{2-}$ and the $CuCl_2$ crystal. Their population analysis of the molecular orbitals led to very low charge transfer between cation and anion in these systems. With the recognition that 4s and 4p orbitals of Cu had their greatest density in the region of the Cl nucleus, a modified electron-counting procedure led to anion and cation charges in accord with Cl^- and Cu^{2+}.

B. Sodium Clusters. Sodium clusters have been examined by CNDO and EH techniques to determine potential energy curves and thereby the most stable geometry. Both procedures generally predict straight chains to be more stable than planar or three-dimensional structures. There is a general increase in BE/n with size, which indicates that aggregation to a larger cluster is energetically favorable. The calculated electronic properties are listed in Tables V and VI.

Experimental values of the sodium-cluster ionization potential are compared with calculated values for linear clusters in Figure 2. The CNDO procedure determined ionization potential by energy difference, and EH employed the highest occupied molecular orbital (HOMO) in accordance with Koopmans' theorem.[29] The EH procedure gives an IP too large by about 1 eV across the series. The CNDO procedure gives an IP too small for odd-size clusters and too large for even-size clusters. It does better for odd-size clusters, but clearly the oscillations are a magnification of the experimental data caused by the calculation. Nevertheless, both calculations indicate no significant trends in IP from the atomic value in this size range. The work function of bulk sodium, 2.3 eV, is not approached by the IP of these small clusters, but the cohesive energy of the bulk, 1.13 eV, is approached by the BE/n data in Tables V and VI. The experimental Na_2 bond length is 3.07 Å[17b] which is considerably less than the equilibrium distance calculated by EH in Table VI and is a definite weakness of the procedure.

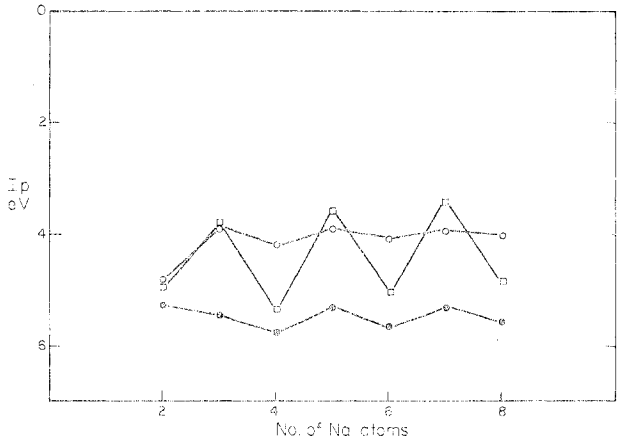

Figure 2. Ionization potential *vs.* size for linear Na clusters: □, CNDO calculation; ●, extended Hückel calculation; ○, experiment.

IV. Conclusions

1. The CNDO procedure parameterized on Cu_2 and Cl_2 yields data in general agreement with experimental values of several electronic properties of $(CuCl)_n$, $n = 1$–5.

2. The most stable calculated $(CuCl)_n$ structure does not correlate with the largest average coordination number of these structures.

3. The electronic properties of small $(CuCl)_n$ clusters are quite different from bulk CuCl properties. The ionization potential and excitation energy are larger for the small clusters, but the bond energy is smaller.

4. Extended Hückel and CNDO calculations predict linear geometry to be generally the most stable geometry of sodium particles. The ionization potential calculated for these particles follows the experimental trends with size.

Registry No. CuCl, 7758-89-6; Cu_2Cl_2, 12258-96-7; Cu_3Cl_3, 11093-65-5; Cu_4Cl_4, 11093-67-7; Cu_5Cl_5, 11093-68-8; Cu_6Cl_6,

12622-24-1; Cu_7Cl_7, 53906-70-0; Cu_8Cl_8, 53906-71-1; $Cu_{12}Cl_{12}$, 53906-72-2; $Cu_{15}Cl_{15}$, 53906-73-3; Na_2, 25681-79-2; Na_3, 37279-42-8; Na_4, 39297-86-4; Na_5, 39297-87-5; Na_6, 39297-88-6; Na_7, 39297-89-7; Na_8, 39297-90-0.

References and Notes

(1) J. A. Pople, D. P. Santry, and G. A. Segal, *J. Chem. Phys.*, **43**, S129 (1965).
(2) R. Hoffmann, *J. Chem. Phys.*, **39**, 1397 (1963).
(3) J. H. Sinfelt, *Chem. Eng. Progr., Symp. Ser.*, **63**, 16 (1967).
(4) J. H. Sinfelt, *J. Catal.*, **29**, 308 (1973).
(5) H. Stoll and H. Preuss, *Phys. Status Solidi*, **53**, 519 (1972).
(6) R. Hoffmann, *Tetrahedron*, **22**, 521 (1966).
(7) H. Dunken, *Z. Chem.*, **12**, 433, 475 (1972).
(8) G. Blyholder, *J. Chem. Soc., Chem. Commun.*, 625 (1973).
(9) R. C. Baetzold, *J. Chem. Phys.*, **55**, 4363 (1971).
(10) R. C. Baetzold, *J. Catal.*, **29**, 129 (1973).
(11) D. J. M. Fassaert, H. Verbeek, and A. Van der Avoird, *Surface Sci.*, **29**, 501 (1972).
(12) J. C. Robertson and C. W. Wilmsen, *J. Vac. Sci. Technol.*, **9**, 901 (1972).
(13) J. C. Robertson and C. W. Wilmsen, *J. Vac. Sci. Technol.*, **8**, 53 (1971).
(14) C. J. Ballhausen and H. B. Gray, *Inorg. Chem.*, **1**, 111 (1962).
(15) M. Guido, G. Balducci, G. Gigli, and M. Spoliti, *J. Chem. Phys.*, **55**, 4566 (1971).
(16) M. Guido, G. Gigli, and G. Balducci, *J. Chem. Phys.*, **57**, 3731 (1972).
(17) (a) E. J. Robbins, R. E. Leckenby, and P. Willis, *Advan. Phys.*, **16**, 739 (1967); (b) P. J. Foster, R. E. Leckenby, and E. J. Robbins, *Proc. Phys. Soc., London (At. Mol. Phys.)*, **2**, 478 (1969).
(18) R. C. Baetzold, *J. Chem. Phys.*, **55**, 4355 (1971).
(19) C. E. Moore, *Nat. Bur. Stand. (U.S.), Circ.*, No. 467 (1949).
(20) E. Clementi and D. L. Raimondi, *J. Chem. Phys.*, **38**, 2686 (1963).
(21) L. C. Cusachs and J. H. Corrington, "Sigma MO Theory," O. Sinanoglu and K. Widberg, Ed., Yale University Press, New Haven, Conn., 1970.
(22) L. C. Cusachs and J. W. Reynolds, *J. Chem. Phys.*, **43**, S160 (1965).
(23) M. Wolfsberg and L. Helmholz, *J. Chem. Phys.*, **20**, 837 (1952).
(24) J. J. Burton, *J. Chem. Phys.*, **52**, 345 (1970).
(25) C. Kittel, "Introduction to Solid State Physics," 3rd ed, Wiley, New York, N.Y., 1968.
(26) F. Herman and D. S. McClure, *Bull. Amer. Phys. Soc.*, **5**, 48 (1960).
(27) S. Kono, T. Ishii, T. Sagawa, and T. Kobayasi, *Phys. Rev. B*, **8**, 795 (1973).
(28) P. Ros and G. C. A. Schuit, *Theor. Chim. Acta*, **4**, 1 (1966).
(29) T. A. Koopmans, *Physica*, **1**, 104 (1933).

Notes

Contribution from the Department of Chemistry, University of Utah, Salt Lake City, Utah 84112

Preparation of Bis(halodifluorophosphine)-Diborane(4) Complexes

R. T. Paine* and R. W. Parry

Received April 16, 1974 AIC40245Z

A few complexes of the bidentate Lewis acid B_2H_4 have been reported. Graybill and Ruff[1] prepared $[(C_6H_5)_3P]_2{\cdot}B_2H_4$ from $(CH_3)_3N{\cdot}B_3H_7$ through the reaction

$$(CH_3)_3N{\cdot}B_3H_7 + 3[(C_6H_5)_3P](\text{excess}) \xrightarrow[50^\circ]{\text{benzene}} [(C_6H_5)_3P]_2{\cdot}B_2H_4 + (C_6H_5)_3P{\cdot}BH_3 + N(CH_3)_3$$

Deever, Lory, and Ritter, in a series of papers, described the preparation of B_2H_4 complexes of PF_3[2,3] and PF_2H[4] from $(CH_3)_2O{\cdot}B_3H_7$

$$(CH_3)_2O{\cdot}B_3H_7 + PF_3(\text{excess}) \xrightarrow{-16^\circ} (F_3P)_2{\cdot}B_2H_4 + F_3P{\cdot}BH_3$$

$$(CH_3)_2O{\cdot}B_3H_7 + PF_2H(\text{excess}) \xrightarrow{-16^\circ} (F_2HP)_2{\cdot}B_2H_4 + F_2HP{\cdot}BH_3$$

Lory and Ritter[4] prepared $(R_2NPF_2)_2{\cdot}B_2H_4$ and $(F_2HP)_2{\cdot}B_2H_4$ using B_4H_{10} as a B_2H_4 source instead of $(CH_3)_2O{\cdot}B_3H_7$. In the present study the bis(ligand)–diborane(4) complexes of PF_2X where X is F, Cl, and Br have been prepared from both $(CH_3)_2O{\cdot}B_3H_7$ and B_4H_{10}. The appropriate equations are

$$3F_2XP + (CH_3)_2O{\cdot}B_3H_7 \xrightarrow[5\text{ hr}]{0^\circ} (F_2XP)_2{\cdot}B_2H_4 + F_2XP{\cdot}BH_3 + (CH_3)_2O$$

$$4F_2XP(\text{excess}) + B_4H_{10}\left(\begin{matrix}H\\H\end{matrix}\!\!\rangle B\langle\!\!\begin{matrix}H\\H\end{matrix}\right)B_3H_6 \xrightarrow[3\text{-}5\text{ days}]{0^\circ} (F_2XP)_2{\cdot}B_2H_4 + 2F_2XP{\cdot}BH_3$$

The reactions involved and the products obtained can be analyzed in terms of base displacement processes which were considered in a general sense by Parry and Edwards[5] and in a more refined sense by Deever, Lory, and Ritter[3] and by Paine and Parry.[6]

Experimental Section

Equipment. Standard high-vacuum techniques were used for the manipulation of the volatile compounds. Infrared spectra were recorded on a Beckman IR20 spectrometer using a 70-mm path length gas cell with KBr windows. The nmr spectra were recorded on a Varian HA/HR 100 instrument operating at 32.1 MHz (^{11}B) and 94.1 MHz (^{19}F).[7] An external standard, $(CH_3)_3B$, was used for the ^{11}B nmr spectrum and an internal standard, $CFCl_3$, was used for the ^{19}F nmr spectrum. The $CFCl_3$ also served as the sample solvent.

Materials. Tetraborane(10) was prepared by the "hot–cold" tube pyrolysis of diborane(6) as described by Klein, Harrison, and Solomon.[8] The $(CH_3)_2O{\cdot}B_3H_7$ samples were prepared and purified as described by Deever and Ritter.[9] Trifluorophosphine was purchased from Ozark Mahoning Co. and was distilled through a −160° trap before using. The F_2ClP and F_2BrP ligands were prepared and purified by literature procedures.[10]

Reaction of B_4H_{10} with F_2XP. A 2.7-mmol sample of B_4H_{10} and a 12.5-mmol sample of F_2XP, X = F, Cl, or Br, were condensed into a 5.0-ml tube and sealed off. The tube was held at 0° for 3–5 days and then opened, and the contents were vacuum distilled through traps held at −96, −126, −160, and −196°. The $(F_3P)_2{\cdot}B_2H_4$ complex was retained at −126° and the $(F_2ClP)_2{\cdot}B_2H_4$ and $(F_2BrP)_2{\cdot}B_2H_4$ complexes were retained at −96°. The complexes were identified by infrared and nmr spectra. The yields of $(F_2XP)_2{\cdot}B_2H_4$ were 50–60% based on the B_4H_{10} consumed. When the same reactions were run in an nmr tube with a reactant ratio of $F_2XP:B_4H_{10}$ = 5:1, the ^{19}F nmr spectra of the products showed $(F_2XP)_2{\cdot}B_2H_4$ and $F_2XP{\cdot}BH_3$, but no $F_2XP{\cdot}B_3H_7$.

Reaction of $(CH_3)_2O{\cdot}B_3H_7$ with Excess F_2XP. A 3.1-mmol sample of $(CH_3)_2O{\cdot}B_3H_7$ was prepared in a 10-ml reaction tube equipped with a Teflon stopcock. A 9.7-mmol sample of F_2XP, X = F, Cl, or Br, was added, the tube was closed, and then the system was held at 0° for 5 hr. After the reaction was complete, the tube was held at −78° and the volatile products were vacuum distilled as described above. The yields of $(F_2XP)_2{\cdot}B_2H_4$ complexes were approximately 40% based on the $(CH_3)_2O{\cdot}B_3H_7$ consumed. When the same reactions were run in an nmr tube with the reactant ratio $F_2XP:(CH_3)_2O{\cdot}B_3H_7$ = 3:1, the ^{19}F nmr spectra of the products showed large amounts of $(F_2XP)_2{\cdot}B_2H_4$ and $F_2XP{\cdot}BH_3$ and a very small amount of $F_2XP{\cdot}B_3H_7$.

Properties of $(F_2XP)_2{\cdot}B_2H_4$ Complexes. The infrared spectra of the $(F_2XP)_2{\cdot}B_2H_4$ complexes were similar to that reported by Deever and Ritter[2] for $(F_3P)_2{\cdot}B_2H_4$. The absorptions (cm^{-1}) and tentative assignments for $(F_2ClP)_2{\cdot}B_2H_4$ are as follows: 2400 [ν_{as}(B–H)], 2350 [ν_s(B–H)], 1100 [$\delta(BH_2)$], 1000 [?], 960 [ν(P–F)], 850 [ν(P–F)], 640 [ν(P–B)], 535 [ν(P–Cl)], 390 [δ(P–F)]. The spectrum of $(F_2BrP)_2{\cdot}B_2H_4$ is identical except for [ν(P–Br)]. (The symbols used above are defined as ν = stretch and δ = deformation.) The ^{11}B and ^{19}F nmr spectral parameters are summarized in the order X = F, Cl,